Moussa, S.; Concepción Heydorn, P.; Arribas Viana, MDLD.; Martinez Feliu, A. (2020). The nature of active Ni sites and the role of Al species in the oligomerization of ethylene on mesoporous Ni-Al-MCM-41 catalysts. Applied Catalysis A General. 608:1-10. https://doi.org/10.1016/j.apcata.2020.117831

Supplementary Material

The nature of active Ni sites and the role of Al species in the oligomerization of ethylene on mesoporous Ni-Al-MCM-41 catalysts

Sara Moussa, Patricia Concepción, Maria A. Arribas, and Agustín Martínez*

Instituto de Tecnología Química, Universitat Politècnica de València - Consejo Superior de Investigaciones Científicas (UPV-CSIC), Avda. de los Naranjos s/n, 46022 Valencia, Spain.

*Corresponding author: amart@itq.upv.es (A. Martínez)

Table S1. Initial (TOS = 1 min) and *pseudo*-steady state (TOS = 60 min) carbon number distribution of oligomers (in wt%) for *x*Ni/Al-M41 catalysts with different Ni content in the ethylene oligomerization experiments performed at 120 °C, 1 bar total presure (0.95 bar ethylene, balanced by Ar), and WHSV of 33 h^{-1}. No products higher than C_8 were found at these reaction conditions.

	1Ni/Al-M41		3Ni/Al-M41		5Ni/Al-M41		10Ni/Al-M41	
	Initial	SS[a]	Initial	SS[a]	Initial	SS[a]	Initial	SS[a]
X_{ethyl}[b] (%)	7.1	2.1	9.0	2.8	10.3	3.1	10.8	3.2
Oligomer distribution (wt%)								
$C_4^=$	88.4	92.0	87.5	91.8	87.8	91.7	87.7	91.4
$C_5^=$	1.5	0.3	1.3	0.2	1.1	0.2	1.1	0.2
$C_6^=$	7.1	6.7	8.1	7.0	8.3	6.8	8.3	7.2
$C_7^=$	0.6	0.0	0.6	0.0	0.5	0.0	0.5	0.0
$C_8^=$	2.4	1.0	2.5	1.0	2.3	1.3	2.4	1.2

[a] SS: *pseudo*-steady state. [b] Conversion of ethylene.

Table S2. Carbon number distribution of oligomers (in wt%) in the *pseudo*-steady state for *x*Ni/Al-M41 catalysts obtained in the high-pressure ethylene oligomerization experiments. Reaction conditions: 120 °C, 35 bar total presure (26 bar ethylene, balanced by Ar), and WHSV of 10 h^{-1}.

Catalyst	1Ni/Al-M41	3Ni/Al-M41	5Ni/Al-M41	10Ni/Al-M41
X_{ethyl} (%)	41.6	77.8	91.2	92.7
Oligomer distribution (wt%)				
$C_4^=$	60.7	56.8	49.8	41.6
$C_5^=$	0.4	0.4	0.5	0.4
$C_6^=$	9.9	13.3	15.5	16.0
$C_7^=$	0.2	0.2	0.2	0.2
$C_8^=$	8.4	11.8	13.7	13.3
$C_9^=$	0.5	0.4	0.4	0.3
$C_{10}^=$	7.3	8.8	10.3	11.8
$C_{11}^=$	0.5	0.2	0.2	0.3
$C_{12}^=$	7.2	4.6	5.1	9.5
$C_{13+}^=$	4.9	3.5	4.3	6.6

Fig. S1. Reproducibility of catalytic experiments at high and ambient pressure conditions over selected *x*Ni/Al-M41 catalysts.

A) Ethylene conversion-TOS curves (a) and product distribution in the steady state (b) at 120 °C, 35 bar, and WHSV of 10 h^{-1} for catalyst 5Ni/Al-M41.

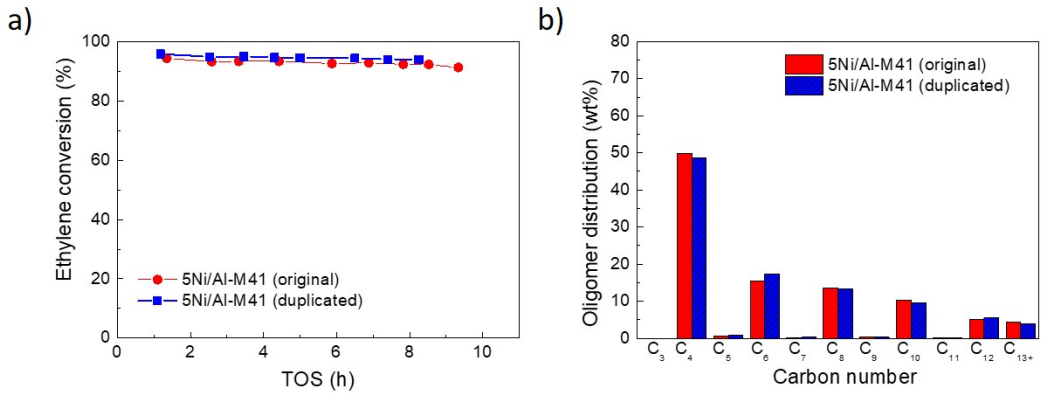

B) Ethylene conversion-TOS curves (a) and product distribution in the steady state (b) at 120 °C, 1 bar, and WHSV of 33 h^{-1} for catalyst 10Ni/Al-M41.

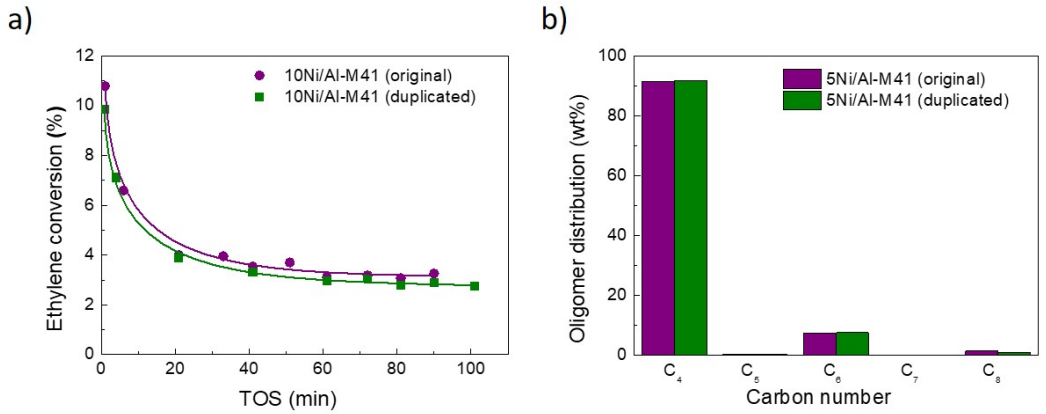

Fig. S2. Low-angle XRD patterns of Al-M41 support and impregnated xNi/Al-M41 catalysts with different Ni loading.

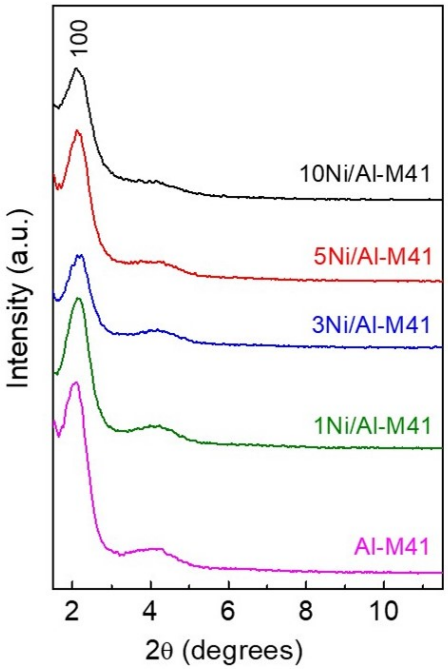

Fig. S3. Nitrogen adsorption isotherms (a) and BJH-KJS pore size distributions (b) for the Al-M41 carrier and *x*Ni/Al-M41 catalysts. For the sake of clarity, the isotherms for samples 1Ni/Al-M41, 3Ni/Al-M41, 5Ni/Al-M41, and 10Ni/Al-M41 have been up-shifted by, respectively, 110, 194, 320, and 451 cm^3/g.

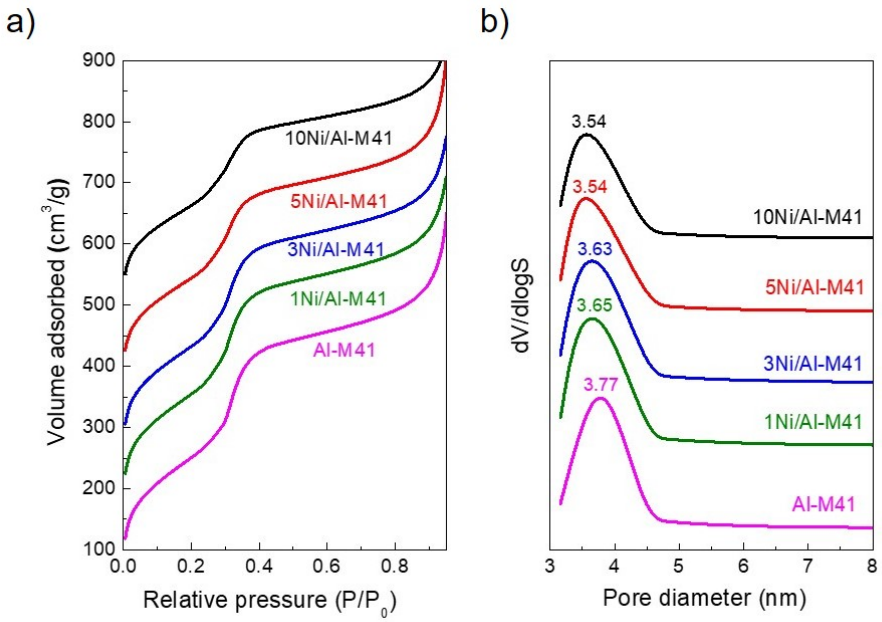

Fig. S4. High-angle XRD patterns of impregnated *x*Ni/Al-41 catalysts with different Ni loadings.

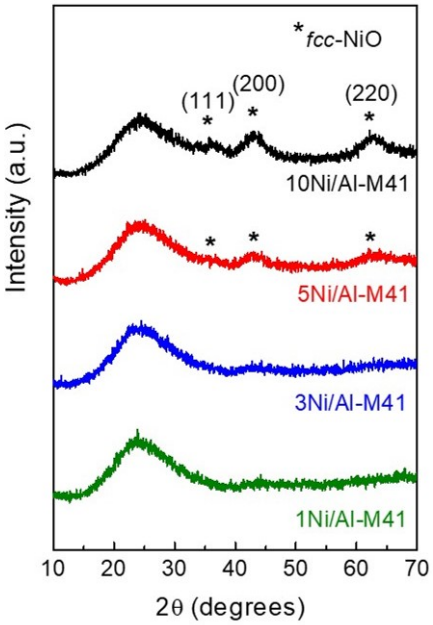

Fig. S5. H_2-TPR profile of NiO crystallites with average particle size of 30 nm physically mixed with the Al-MCM-41 support to obtain a Ni content of 5 wt%.

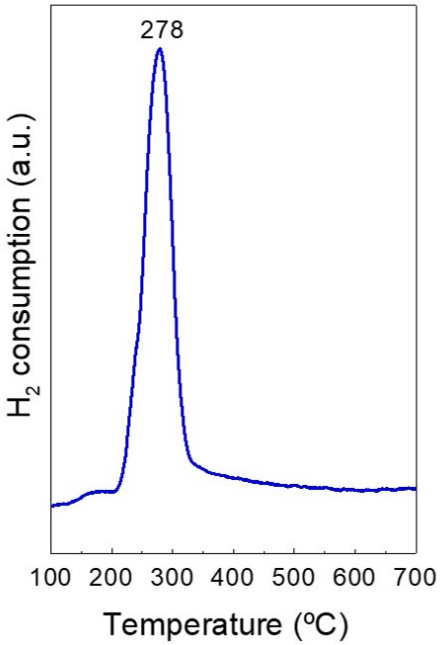

Fig. S6. Deconvoluted H_2-TPR profiles for catalysts 1Ni/Al-M41 (1.3 wt% Ni), 3Ni/Al-M41 (2.8 wt% Ni), and 5Ni/Al-M41 (5.7 wt% Ni).

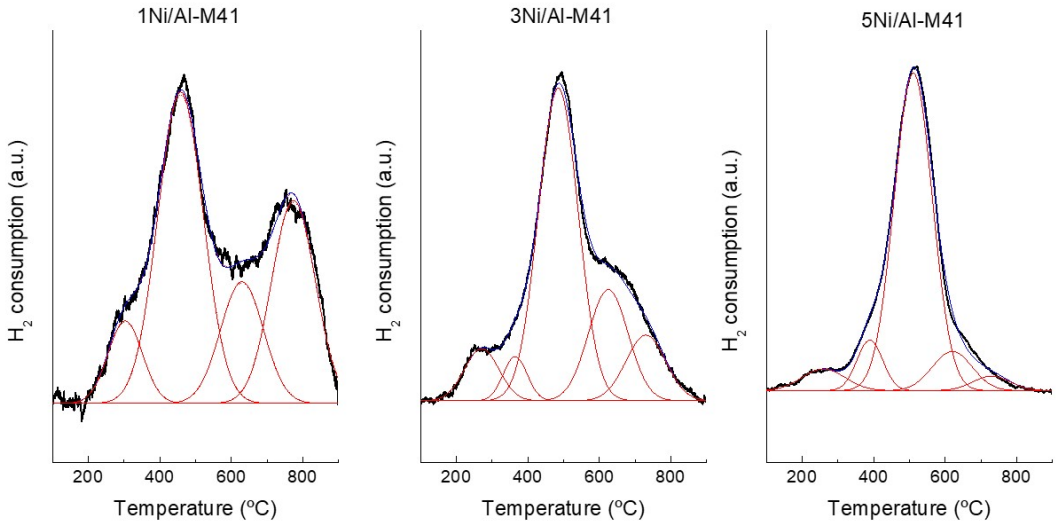

Fig. S7. TEM image of NiO nanoparticles in the impregnated 1Ni/Al-M41 catalyst with Fast Fourier Transform (FFT) analysis of a selected nanoparticle.

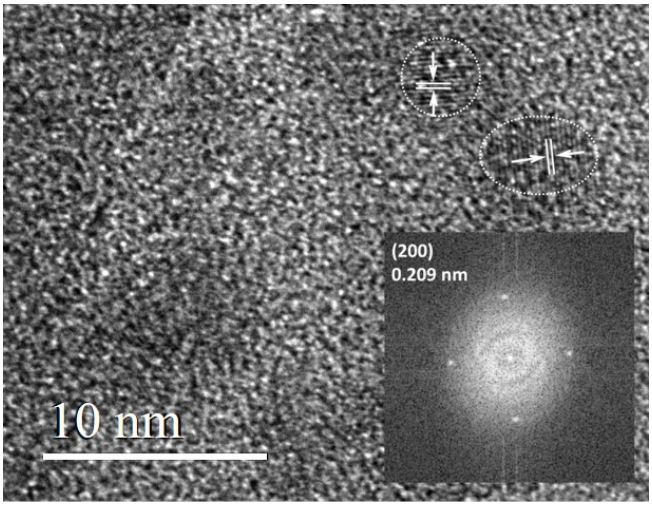

A lattice spacing of 0.209 nm was determined by FFT, in line with the theoretical value (0.2084 nm) of the (200) plane of *fcc*-NiO nanoparticles.

Fig. S8. a) FTIR spectra of adsorbed CO at increasing CO dosing (0.14 – 2.0 mbar) for the impregnated 5Ni/Al-M41 sample; b) second derivative curves for selected spectra.

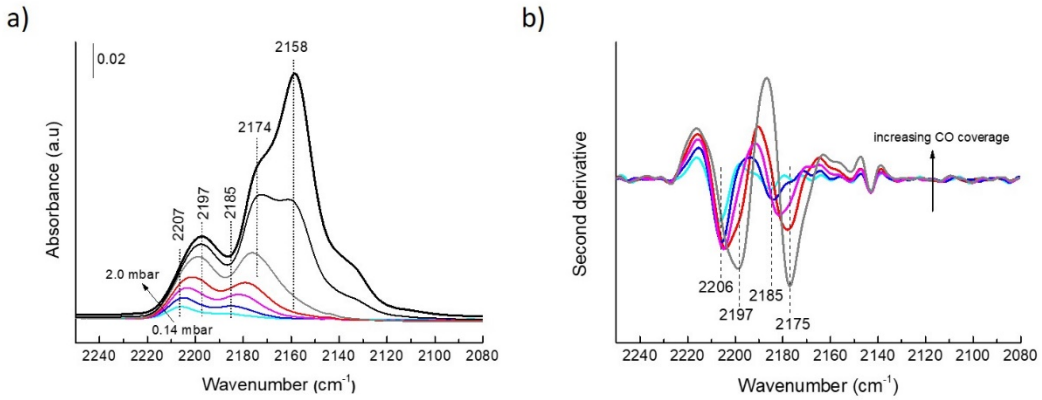

Fig. S9. Deconvoluted FTIR-CO spectrum at CO saturation of Ni-carbonyls of an Al-free Ni-Si-M41 sample (1.7 wt% Ni) prepared by grafting (see main text) after thermal treatment in flowing N_2 at 300 ºC. Only the region of Ni-carbonyls is shown for the sake of clarity.

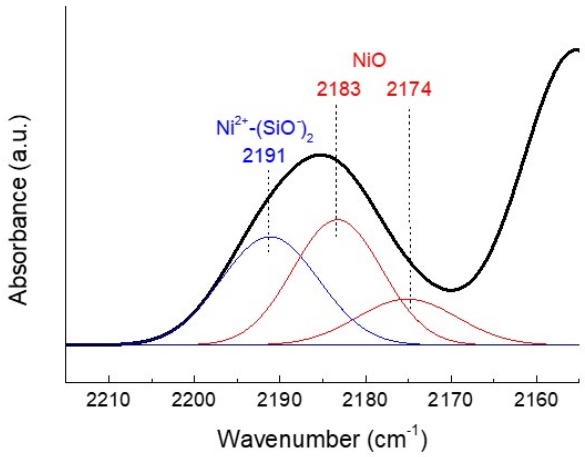

Fig. S10. Evolution with Ni loading of the integrated area of the different Ni^{2+}-CO IR bands (ion-exchanged: 2207 cm^{-1}, grafted on silanols: 2197 cm^{-1}, NiO: 2185 cm^{-1}) for thermally treated (N_2, 300 °C) *x*Ni/Al-M41 catalysts assessed from the deconvoluted IR spectra at CO saturation of Ni-carbonyl bands.

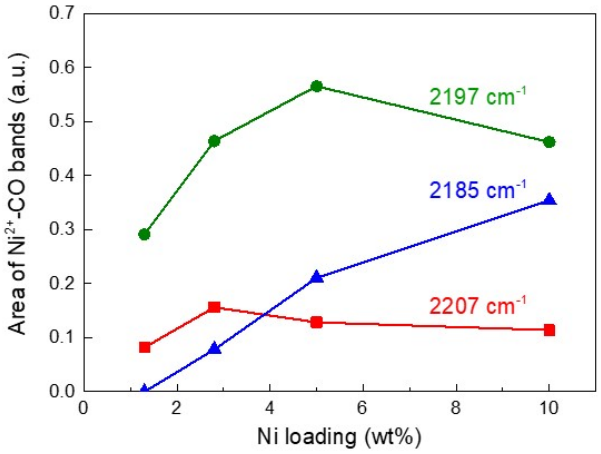

Fig. S11. Ethylene conversion rate as a function of TOS (a) and of Ni loading at TOS of 1 min and > 60 min (b) for *x*Ni/Al-M41 catalysts. Reaction conditions: 120 °C, 1 bar total pressure (0.95 bar ethylene + 0.05 bar Ar), and WHSV of 33 h^{-1}.

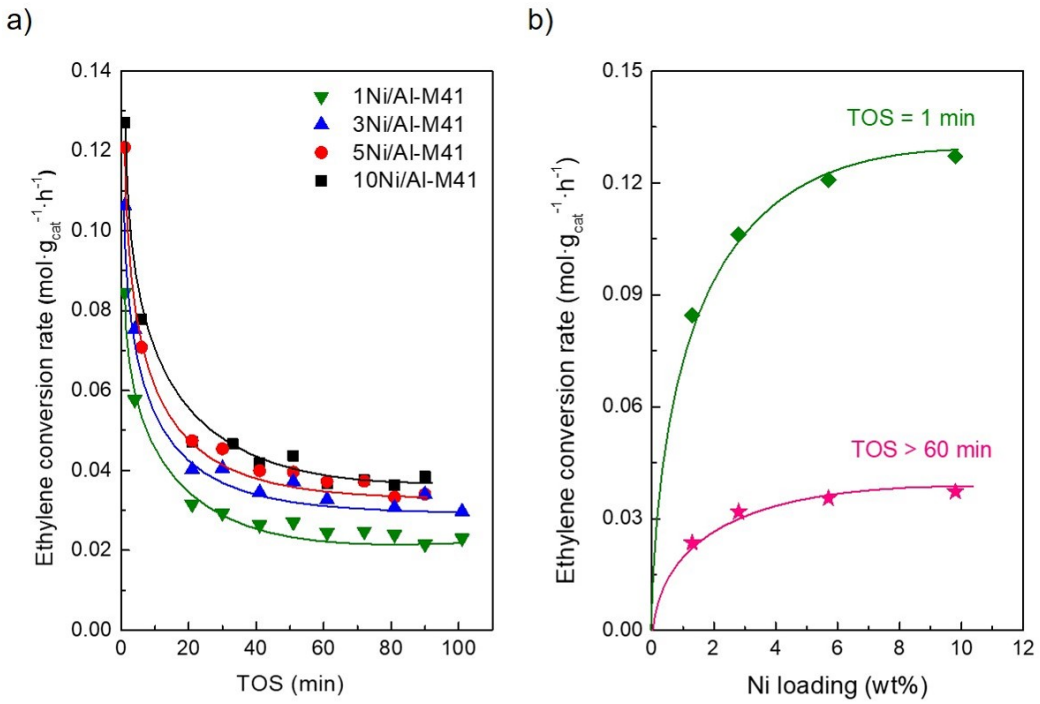

Fig. S12. Evolution of ethylene conversion with TOS for *x*Ni/Al-M41 catalysts at 120 °C, 35 bat total pressure (26 bar ethylene), and WHSV of 10 h^{-1}.

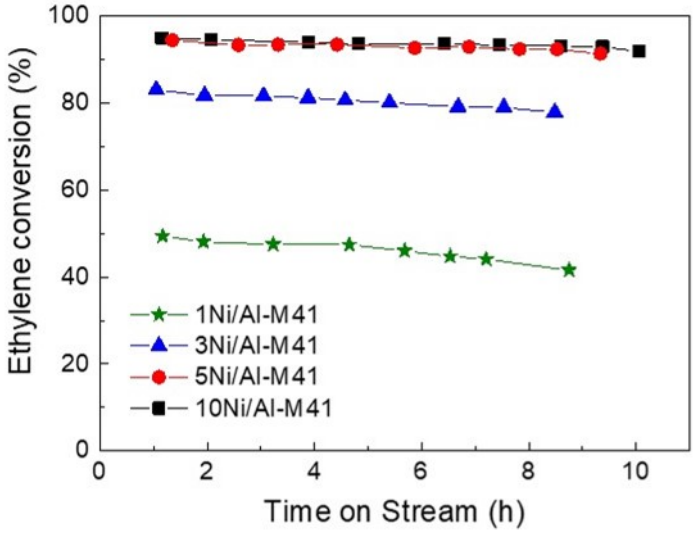

Fig. S13. (a) FTIR spectrum at CO saturation of Ni-carbonyl bands for 5Ni/Al-M41 catalyst after 70 min of in situ reaction with ethylene at 120 °C and 1 bar, and (b) second derivative curve.

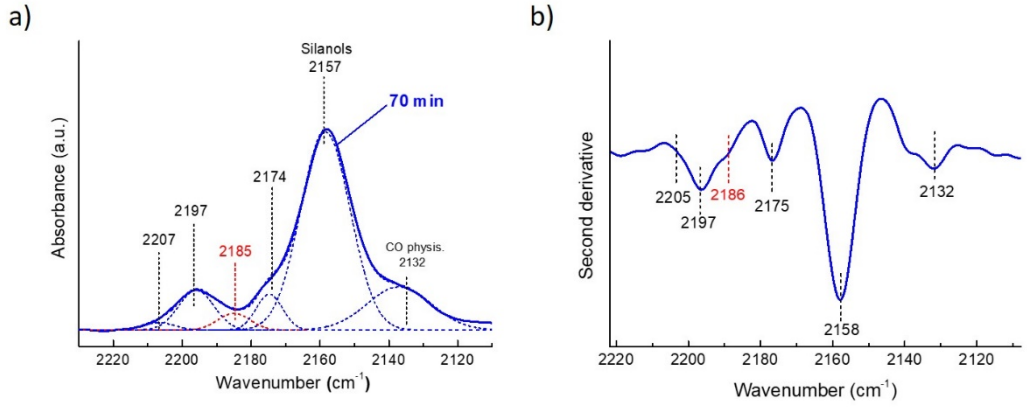

Fig. S14. FTIR spectra at CO saturation of Ni-carbonyl bands for 3Ni/Al-M41 catalyst after the pretreatment in N_2 at 300 °C (0 min) and after 70 min of in situ reaction with ethylene at 120 ºC and 1 bar.

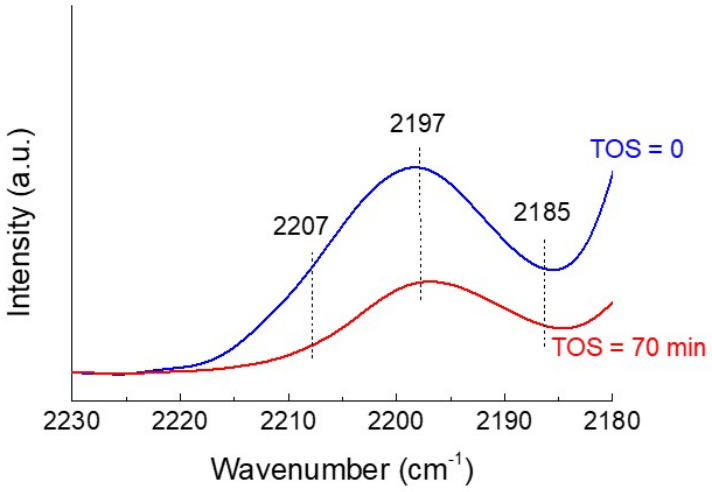

Fig. S15. FTIR spectra in the C-H stretching (a) and bending (b) vibration regions for the 5Ni/Al-M41 catalyst after the thermal treatment at 300 °C (0 min) and after reaction with ethylene at 120 ºC and 1 bar for 1 and 70 min and subsequent evacuation of the cell at 120 ºC for 1 h under dynamic vacuum of 10^{-5} mbar. The IR spectra were normalized by sample overtone area.

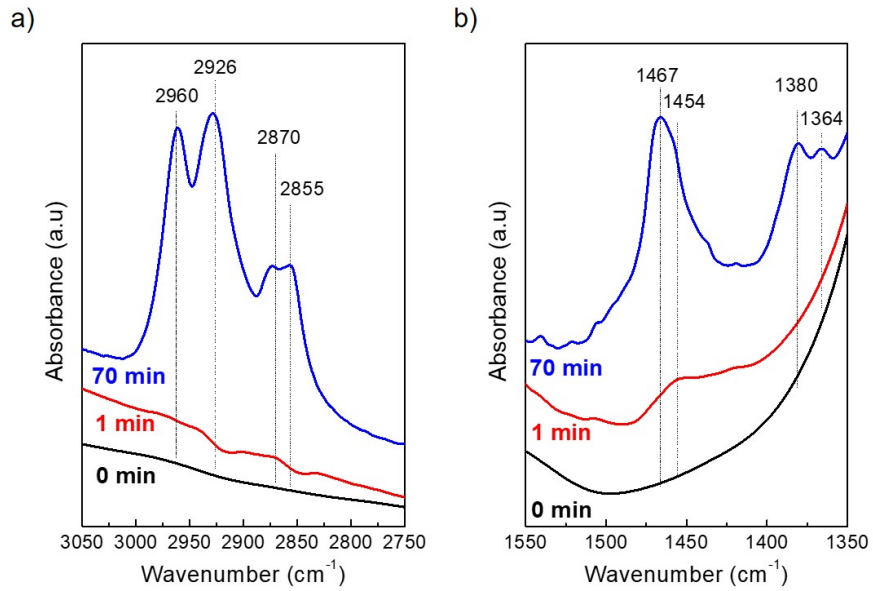

As shown in the figures, characteristic C-H stretching and bending IR bands of CH_3 (ν_{as}= 2960 cm^{-1}, ν_s= 2870 cm^{-1}, δ_s= 1364 – 1380 cm^{-1}, δ_{as}= 1440 – 1470 cm^{-1}) and CH_2 (ν_{as}= 2926 cm^{-1}, ν_s= 2855 cm^{-1}, δ= 1440 – 1470 cm^{-1}) groups are observed.

Fig. S16. Low- (a) and high-angle (b) XRD patterns of Ni catalysts grafted on silica materials: Ni-Si-M41 (1.7 wt% Ni) and NiO-SiO_2 (2.7 wt% Ni).

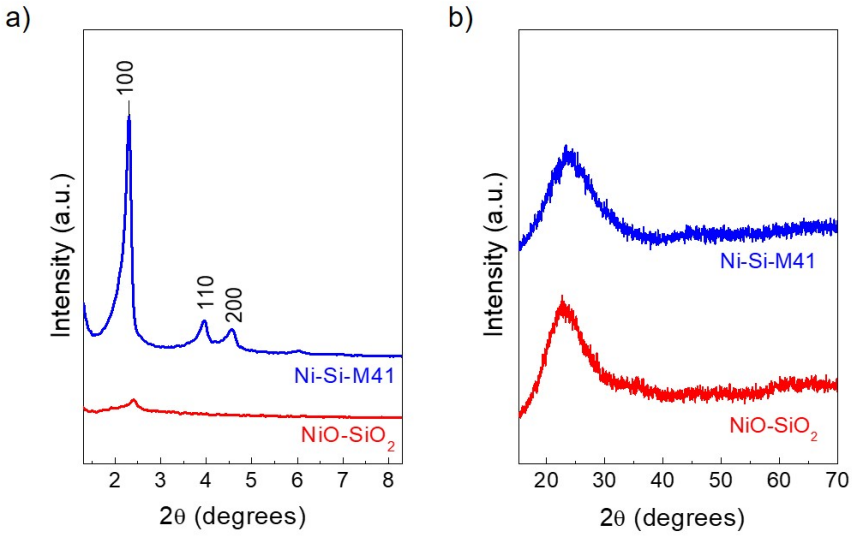

Fig. S17. Representative STEM image showing the presence of small (2 – 5 nm) NiO nanoparticles in the Al-free NiO-SiO_2 sample.